Video Article

Ultrasonic Assessment of Myocardial Microstructure

Pranoti Hiremath[1], Michael Bauer[2], Hui-Wen Cheng[2], Kazumasa Unno[2], Ronglih Liao[2], Susan Cheng[2]

[1]Harvard Medical School

[2]Cardiovascular Division, Department of Medicine, Brigham and Women's Hospital, Harvard Medical School

Correspondence to: Susan Cheng at scheng3@partners.org

URL: https://www.jove.com/video/50850
DOI: doi:10.3791/50850

Keywords: Medicine, Issue 83, echocardiography, image analysis, myocardial fibrosis, hypertension, cardiac cycle, open-access image analysis software

Date Published: 1/14/2014

Citation: Hiremath, P., Bauer, M., Cheng, H.W., Unno, K., Liao, R., Cheng, S. Ultrasonic Assessment of Myocardial Microstructure. *J. Vis. Exp.* (83), e50850, doi:10.3791/50850 (2014).

Abstract

Echocardiography is a widely accessible imaging modality that is commonly used to noninvasively characterize and quantify changes in cardiac structure and function. Ultrasonic assessments of cardiac tissue can include analyses of backscatter signal intensity within a given region of interest. Previously established techniques have relied predominantly on the integrated or mean value of backscatter signal intensities, which may be susceptible to variability from aliased data from low frame rates and time delays for algorithms based on cyclic variation. Herein, we describe an ultrasound-based imaging algorithm that extends from previous methods, can be applied to a single image frame and accounts for the full distribution of signal intensity values derived from a given myocardial sample. When applied to representative mouse and human imaging data, the algorithm distinguishes between subjects with and without exposure to chronic afterload resistance. The algorithm offers an enhanced surrogate measure of myocardial microstructure and can be performed using open-access image analysis software.

Video Link

The video component of this article can be found at https://www.jove.com/video/50850/

Introduction

Echocardiography is a widely accessible imaging modality that is commonly used to noninvasively characterize and quantify changes in cardiac structure and function. Ultrasonic assessments of cardiac tissue can include analyses of backscatter signal intensity within a given region of interest at a single point in time, as well as over the course of the cardiac cycle. Prior studies have suggested that measures of sonographic signal intensity can identify the underlying presence of myocardial fiber disarray, viable versus nonviable myocardial tissue, and interstitial fibrosis[1-3]. We refer to myocardial 'microstructure' as the tissue architecture that can be characterized, using sonographic analysis, beyond linear measurements of gross size and morphology. Accordingly, analyses of sonographic signal intensity have been used to evaluate microstructural alterations of myocardial tissue in the setting of hypertrophic and dilated cardiomyopathy[4,5], chronic coronary artery disease[6,7], and hypertensive heart disease[8,9]. However, previously established techniques have relied predominantly on the integrated or mean value of backscatter signal intensities, which may be susceptible to variability from random noise[5], aliased data from low frame rates[10], and time delays for algorithms based on cyclic variation[11].

Herein, we describe the method of using an ultrasound-based image analysis algorithm that extends from previous methods; this algorithm focuses on a single end-diastolic frame for image analysis and accounts for the full distribution of signal intensity values derived from a given myocardial sample. By using the pericardium as an in-frame reference[12,13], the algorithm reproducibly quantifies variation in sonographic signal intensity distributions and offers an enhanced surrogate measure of myocardial microstructure. In a step-by-step protocol, we describe methods for preparing images for use, sampling regions of interest, and processing data within selected regions of interest. We also show representative results from applying the algorithm to echocardiographic images acquired from mice and humans with variable exposure to afterload stress on the left ventricle.

Protocol

1. Preparation of Images for Analyses

1. Obtain murine or human echocardiographic B-mode images in the parasternal long-axis view. Adjust time-gain compensation settings and placement of the transmit focus to optimize visualization of the LV and other cardiac structures in the parasternal view, per usual practice. Ensure all images are saved in DICOM file format. Standardized image views place the inferolateral left ventricular wall at the base of the frame. Frames must display the entirety of the left ventricular myocardium and pericardium. Resolution must be high enough to demarcate the pericardial border, myocardial wall, and endocardial border of the left ventricle. Discard images with excess dropout or image artifacts.
2. Import an image file for analysis into ImageJ software platform v1.46 as a DICOM file. Convert the file to an 8-bit image file.

3. Scroll through consecutive frames of the cardiac cycle until reaching an appropriate quality end-diastolic frame. Alternatively, select the end-diastolic frame in an echocardiographic viewing program and then export to a high-resolution .jpg file format for use in ImageJ. Identify the frames closest to end-diastole using the R wave of the ECG tracing, and then identify the single best frame that captures the LV with maximal internal dimension. Consider this single frame the end-diastolic frame.
4. It is suggested that users be blinded to subject identity when selecting regions of interest.

2. ROI Sampling

1. Pericardial reference selection. When selecting the pericardial region of interest (ROI), aim to capture the heterogeneity of the pericardial tissue. Note that image brightness and contrast may be adjusted for ROI selection, as needed, without any effect on analysis results.
    1. Using ImageJ's rectangle drawing tool, select a rectangle with length approximating the middle third of the basal inferolateral pericardial wall.
    2. Resize the rectangular ROI to span the width of the pericardium using the ROI sizing tool.
    3. Rotate the ROI to lie within the pericardial region using ImageJ's rotate tool.
    4. Make any necessary adjustments to the corners of the pericardial ROI. Capture a final pericardial region of interest that lies within the middle third of the pericardial wall, and includes the width of the pericardial wall without extending into the myocardial or extra-cardiac regions. Aim to capture the same relative location and percentage of total pericardial area for all measures made in a given study.
    5. Apply the algorithm to the selection via ImageJ analysis tools (see section 3).

2. Myocardial selection. Once again, aim to capture the heterogeneity of the myocardial tissue within the middle third of the basal inferolateral myocardial wall. Note that image brightness and contrast may be adjusted for ROI selection, as needed, without any effect on analysis results.
    1. Select a rectangle that spans the width of the myocardial wall, excluding the endocardium and epicardium. Ensure that the myocardial selection lies adjacent to the pericardial selection and at the same theta angle. Do not include areas of papillary muscle within the selection area.
    2. Rotate the myocardial ROI such that it lies parallel to the pericardial selection.
    3. Make any necessary adjustments to the corners of the myocardial ROI. Isolate a final myocardial region of interest that lies within the middle third of the myocardial wall, and captures the width of the wall without extending into the pericardial or intraluminal regions.
    4. Apply the algorithm to the selection via an ImageJ macro.

3. Data Analysis and Processing

1. Install the ImageJ macro called "getHistogramValues.txt".
2. Use the ImageJ histogram analysis tool to preview the distribution of signal intensity values within the ROI (perform this step for the pericardial selection and for the myocardial selection).
3. Use the ImageJ macro to record these signal density values for the ROI (perform this step for the pericardial selection and for the myocardial selection).
    1. Assign an intensity value from 0 (darkest) to 255 (brightest) units to each pixel within the selection.
    2. Arrange the intensity values hierarchically, in order of increasing intensity, to produce a distribution of signal intensity.
    3. Select and report the following percentile values for the distribution: 20^{th} percentile, 50^{th} percentile (median), and 80^{th} percentile.

4. Normalize myocardial intensities using the pericardial reference.
    1. Normalize by dividing the myocardial percentile values of intensity by the corresponding pericardial percentile values of intensity[12], or by subtracting the myocardial percentile value of intensity from the pericardial percentile value of intensity[13].
    2. Report values for the four analytic methods: normalized myocardial-to-pericardial values for the 20^{th} percentile, 50^{th} percentile (median), and 80^{th} percentile values.

4. Quantifying Cyclical Variability

1. Apply algorithm to myocardial selections through consecutive frames of the DICOM file, moving through the cardiac cycle. Compare differences in intensity distributions between frames, with attention to end-systolic and end-diastolic frames.
   All the image analyses described above are performed offline on noninvasive echocardiographic images previously acquired and digitally stored in DICOM format. All study protocols were approved by the Brigham and Women's institutional review board and the Harvard Medical Area standing Institutional Animal Care and Use Committee.

Representative Results

Signal intensity analysis is performed in 4 main steps (**Figure 1**), including: 1) image selection and formatting, 2) sampling ROI and reference areas, 3) algorithm application, and 4) processing final values to yield myocardial-to-pericardial intensity ratios. Selection and size of the ROI is standardized to limit interuser as well as intrauser variability (**Figure 2**). The positioning of each ROI is also standardized with respect to each subject's anatomical structures to limit intersubject as well as intrasubject variability.

As a measure of myocardial density, the algorithm is expected to reveal changes in signal intensity throughout the cardiac cycle, corresponding to the anticipated increase in myocardial density in systole compared to diastole. As shown in **Figure 3**, higher percentile values of signal

intensity accentuate cyclical variability in mice with and without 7 weeks of exposure to afterload resistance (*i.e.* a mouse that underwent ascending aortic constriction compared to a vehicle control mouse that underwent sham surgery).

From analysis of a single end-diastolic frame (**Figure 4**), significant differences are also noted for both mouse and human subjects exposed to chronic afterload stress (cases) compared to their representative counterparts (controls). Both the range and magnitude of signal intensity differs between cases and controls. As seen in analyses of cyclic variability, 80th compared to 50th percentile values within each signal intensity distribution suggest a greater relative difference in signal intensity between cases and controls.

The algorithm presented herein provides output in the form of myocardial-to-pericardial ratios of signal intensity, where the pericardial values serve as the in-frame referent (**Figure 5**). The myocardial-to-pericardial signal intensity ratio was determined based on single-frame analysis of images acquired from representative controls and cases of afterload stress. Concordant with the results above, the myocardial-to-pericardial ratio of 80th percentile signal intensity values offers the greatest ability to differentiate between controls and cases. Expected differences in myocardial microstructure, based on our image analysis results, were consistent with findings from myocardial tissue histology in control and case mice at 7 weeks following sham or aortic-banding surgery, respectively (**Figure 6**).

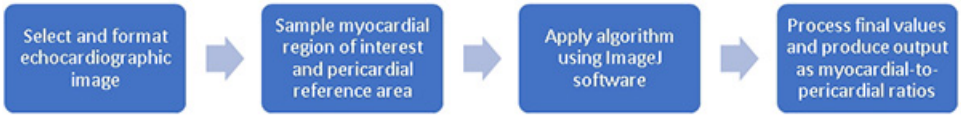

Figure 1. Workflow process for an individual image. The process includes four main steps that may be repeated when comparing subjects or when quantifying cyclical variability. Click here to view larger image.

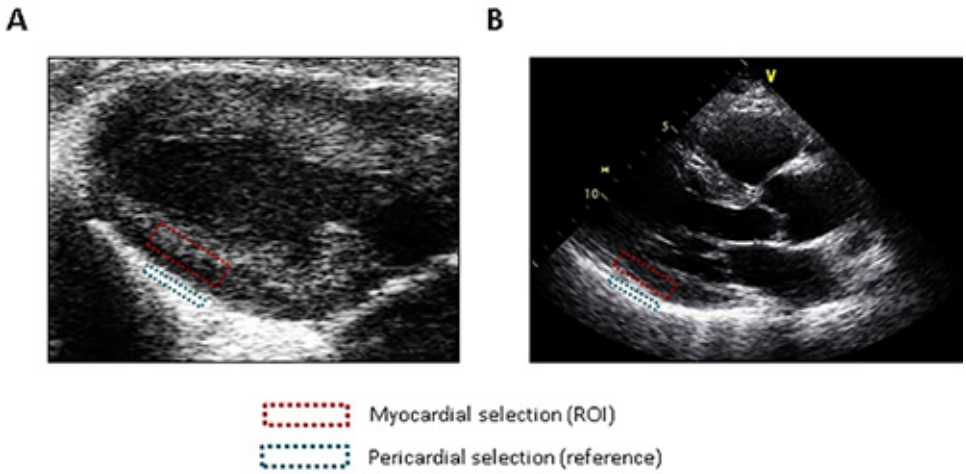

Figure 2. Region of interest (ROI) sampling technique. The image analysis algorithm is standardized for application in mice (**A**) and in humans (**B**). Myocardial and pericardial selections for representative mouse and human images, respectively, are shown. Click here to view larger image.

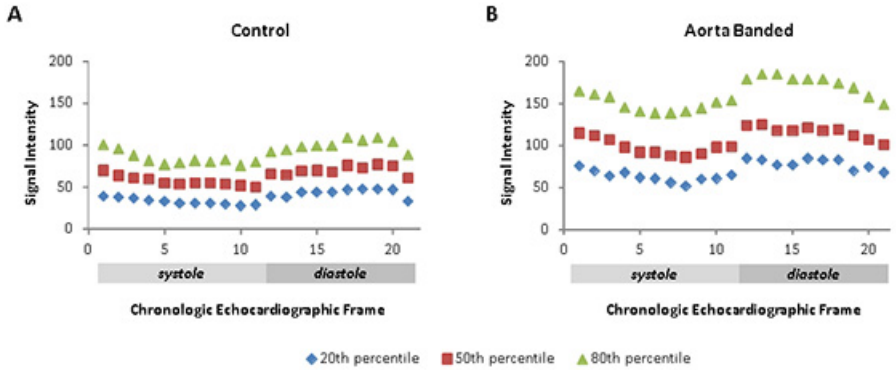

Figure 3. Variation of sonographic signal intensity throughout the cardiac cycle. The algorithm was applied to a myocardial region of interest over consecutive frames of DICOM images acquired from a representative control mouse (**A**) and an aortic-banded mouse (**B**). Frame rate was 212 for both images. For these images, cyclical variability was assessed using 3 cutpoints: 20th percentile (diamond), 50th percentile (square), and 80th percentile (triangle). Relative cyclical variability is higher for the 80th percentile values than for the lower cutpoint values. Click here to view larger image.

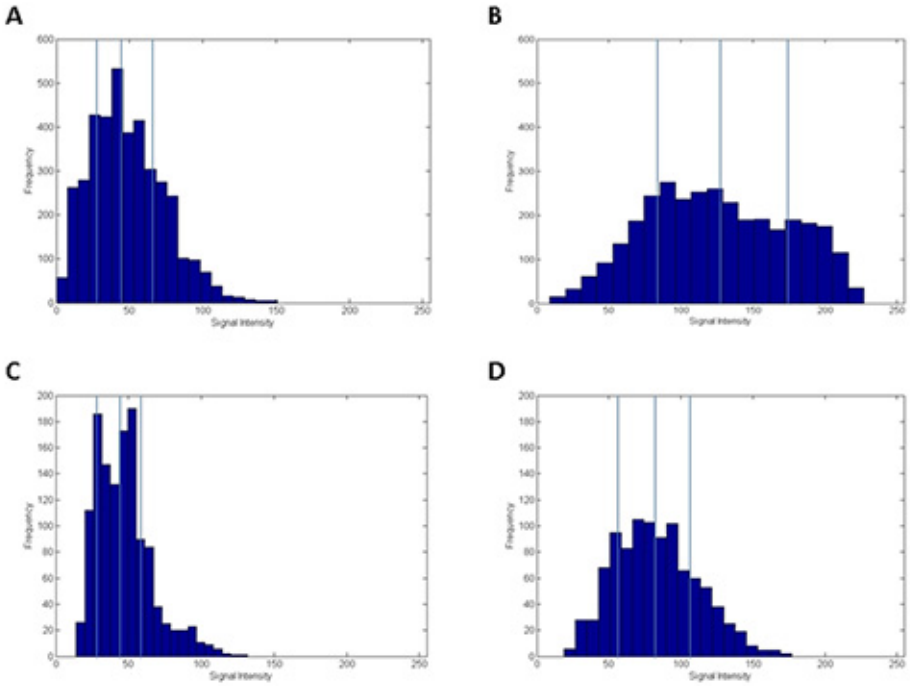

Figure 4. Signal intensity distributions are shown from single-frame analysis of representative mouse and human images. The histograms display distributions of signal intensity derived from myocardium of a control mouse at 7 weeks after sham surgery (**A**), an aortic-banded mouse at 7 weeks after surgery (**B**), a normotensive human (**C**), and a hypertensive human (**D**). Blue vertical lines denote 20th percentile, 50th percentile, and 80th percentile values. The distributions of signal intensity are right-shifted, and are larger in range, for the subjects with chronic afterload stress (*i.e.* aortic-banded compared to control mouse, and hypertensive compared to normotensive human). Click here to view larger image.

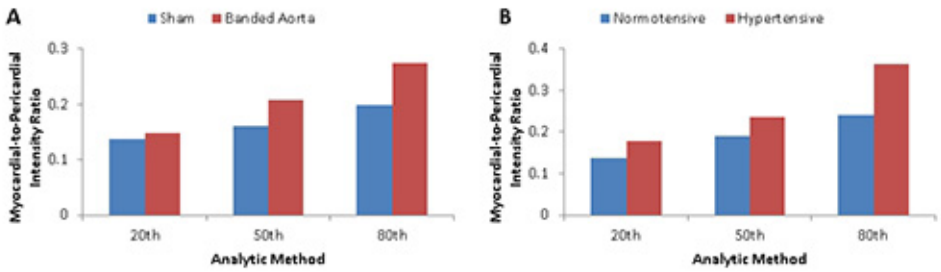

Figure 5. Representative data produced by the image analysis algorithm. (**A**) shows data from a sham-operated (control) compared to aortic-banded (case) mouse at 7 weeks. (**B**) shows data from a human with normal blood pressure (control) compared to a human with chronic hypertension (case). The myocardial-to-pericardial signal intensity ratio was determined using 3 analytic methods within the algorithm: ratio of 20th percentile values; ratio of 50th percentile values; and ratio of 80th percentile values. The greatest difference between controls and cases is demonstrated by using ratios of the 80th percentile values of signal intensity. Click here to view larger image.

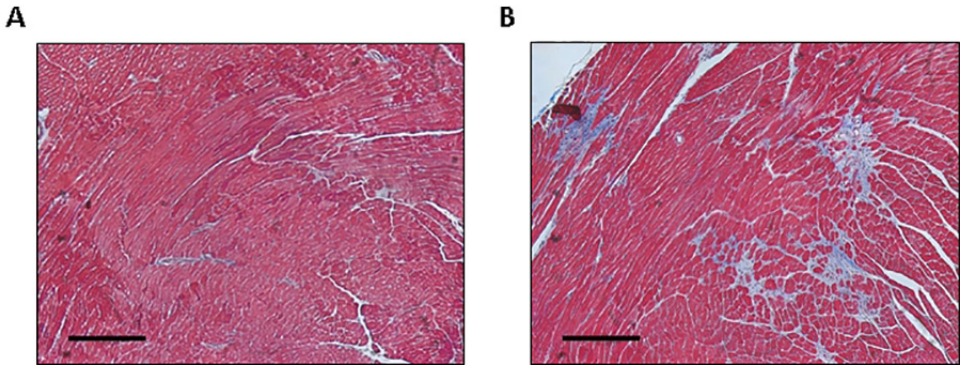

Figure 6. Differences in myocardial tissue histology between mice with and without exposure to afterload stress. Representative Masson's trichrome stained sections of the left ventricle are shown for a mouse that underwent sham surgery (**A**: control) and a mouse that underwent aortic banding (**B**: case) at 7 weeks after surgery. Sections show presence of substantial collagen deposition and interstitial fibrosis in the case compared to the control. Scale bars represent 50 µm. Click here to view larger image.

Discussion

We describe the protocol for an image analysis algorithm that quantifies sonographic signal intensity distribution and, in turn, offers a surrogate measure of myocardial microstructure. Standardized features of the protocol, including selection, sizing, and positioning of the ROI and reference region, serve to minimize user- and subject-based variability. We demonstrate that when applied to end-diastolic single-frame echocardiographic images, the algorithm can appropriately distinguish between normal myocardium versus myocardium exposed to afterload stress.

The protocol details how the algorithm can be employed using the open-source ImageJ software package. Within this image analysis environment, the algorithm can be used to produce data on the distribution of signal intensity values from a given myocardial tissue sample. The resulting signal intensity distributions can be displayed in the form of histograms. Histograms of intensity values within myocardial selections show that diseased myocardial tissues demonstrate a right shift in distribution, and a greater range of values, when compared to nondiseased myocardium. This pattern is seen when the algorithm is applied to both human and murine echocardiographic images.

Variability in signal intensity over the cardiac cycle is observed to correspond with physiological changes in myocardial density. An analytic method that consistently distinguishes density changes throughout the cardiac cycle is believed to be sensitive to differences in myocardial density that occur in response to pathological processes[1,6]. Indeed, cyclical variability is observed upon application of the algorithm to consecutive frames within murine echocardiograms. A larger variation in intensity over the cardiac cycle is observed for imaging intensity values at higher compared to lower percentiles within the total signal intensity distribution.

When the algorithm is applied to representative samples of echocardiographic images acquired from subjects with and without exposure to afterload resistance, the myocardial-to-pericardial ratio density at selected percentile values is observed to be particularly effective at distinguishing subjects with compared to without exposure to chronic afterload resistance. This finding is observed in analyses of representative mouse and human data. Elevated myocardial densities are expected to be seen in the myocardial tissue of subjects exposed to chronic afterload stress, since such stress is known to promote interstitial collagen deposition and the development of myocardial fibrosis[14]. Measurement of myocardial tissue alterations over time could be used to provide a better understanding of the tissue response to prolonged stress and disease progression. Further studies are needed to evaluate if variations in signal intensity correlate with histologic changes over time as well as with increasing severity of a given disease phenotype.

The image analysis algorithm has limited applicability to images with artifacts that would interfere with ROI and/or reference selection, incomplete visualization of the endocardial borders, or overall poor quality. The algorithm may not be able to accurately compare myocardial and pericardial regions of interest when percentile values demonstrate a nonlinear pattern upon grayscale mapping, or when insufficient dynamic range is employed. Although such instances are expected to be rare within the 10^{th} to the 90^{th} percentile values of signal intensity in most phenotypes, preliminary assessment of backscatter linearity and dynamic range may be warranted for studying new phenotypes of interest and/or analyzing images acquired using unconventional ultrasound techniques. The algorithm is also limited by lack of automation of the ROI and reference sample selection process. Additionally, the algorithm has limited capacity for use in cross-comparisons of images captured using markedly different echocardiographic acquisition parameters. In the current report, images in mice were acquired using a 18-38 MHz transducer at frame rates ranging from 225-247 fps; images in humans were acquired using a 1-5 MHz transducer at frame rates ranging from 34-54 fps. Further studies are needed to determine possible protocol revisions that may be required for images acquired using different equipment and at frame rates in marked excess of the above reported ranges.

Disclosures

No conflicts of interest declared.

Acknowledgements

We are grateful for resources provided by the Harvard Medical School/Brigham and Women's Hospital Cardiovascular Physiology Core Laboratory. This work was supported in part by funding from the National Institutes of Health grants HL088533, HL071775, HL093148, and

HL099073 (RL). MB was a recipient of an American Heart Association founder affiliate postdoctoral fellowship award. KU is a recipient of an American Heart Association founders affiliate postdoctoral fellowship award. SC was supported by an award from the Ellison Foundation.

References

1. Yamada, S. & Komuro, K. Integrated backscatter for the assessment of myocardial viability. *Curr. Opin. Cardiol.* **21**, 433-437 (2006).
2. Mimbs, J. W., O'Donnell, M., Bauwens, D., Miller, J. W. & Sobel, B. E. The dependence of ultrasonic attenuation and backscatter on collagen content in dog and rabbit hearts. *Circ. Res.* **47**, 49-58 (1980).
3. Picano, E. *et al. In vivo* quantitative ultrasonic evaluation of myocardial fibrosis in humans. *Circulation.* **81**, 58-64 (1990).
4. Mizuno, R. *et al.* Myocardial ultrasonic tissue characterization for estimating histological abnormalities in hypertrophic cardiomyopathy: comparison with endomyocardial biopsy findings. *Cardiology.* **96**, 16-23, doi:47381 (2001).
5. Mizuno, R., Fujimoto, S., Saito, Y. & Nakamura, S. Non-invasive quantitation of myocardial fibrosis using combined tissue harmonic imaging and integrated backscatter analysis in dilated cardiomyopathy. *Cardiology.* **108**, 11-17, doi:10.1159/000095595 (2007).
6. Marini, C. *et al.* Cyclic variation in myocardial gray level as a marker of viability in man. A videodensitometric study. *Eur. Heart. J* **17**, 472-479 (1996).
7. Komuro, K. *et al.* Sensitive detection of myocardial viability in chronic coronary artery disease by ultrasonic integrated backscatter analysis. *J. Am. Soc. Echocardiogr.* **18**, 26-31, doi:10.1016/j.echo.2004.08.019 (2005).
8. Ciulla, M. *et al.* Echocardiographic patterns of myocardial fibrosis in hypertensive patients: endomyocardial biopsy versus ultrasonic tissue characterization. *J. Am. Soc. Echocardiogr.* **10**, 657-664 (1997).
9. Maceira, A. M., Barba, J., Varo, N., Beloqui, O. & Diez, J. Ultrasonic backscatter and serum marker of cardiac fibrosis in hypertensives. *Hypertension.* **39**, 923-928 (2002).
10. D'Hooge, J. *et al.* High frame rate myocardial integrated backscatter. Does this change our understanding of this acoustic parameter? *Eur. J. Echocardiogr.* **1**, 32-41, doi:10.1053/euje.2000.0004 (2000).
11. Finch-Johnston, A. E. *et al.* Cyclic variation of integrated backscatter: dependence of time delay on the echocardiographic view used and the myocardial segment analyzed. *J. Am. Soc. Echocardiogr.* **13**, 9-17 (2000).
12. Di Bello, V. *et al.* Increased echodensity of myocardial wall in the diabetic heart: an ultrasound tissue characterization study. *J. Am. Coll. Cardiol.* **25**, 1408-1415, doi:10.1016/0735-1097(95)00026-Z (1995).
13. Takiuchi, S. *et al.* Quantitative ultrasonic tissue characterization can identify high-risk atherosclerotic alteration in human carotid arteries. *Circulation.* **102**, 766-770 (2000).
14. Querejeta, R. *et al.* Serum carboxy-terminal propeptide of procollagen type I is a marker of myocardial fibrosis in hypertensive heart disease. *Circulation.* **101**, 1729-1735 (2000).

